Limits on Antiprotons in Space from the Shadowing of Cosmic Rays by the Moon

Presented by: Yupeng Xu
(ETH Zürich / L3+C collaboration)

PhD Students Seminar, PSI, October 1-2, 2003

- The L3+C Experiment
- Motivation: Antiprotons in space
- The Earth-Moon system as a spectrometer
- The angular resolution
- $\overline{p}/p$ ratio: measurement and limits
- Summary and outlook

2nd part:
Measurement of the atmospheric muon spectrum from 20 to 2000 GeV

The L3+C experiment

- Location: 6.02°E, 46.25°N, 450 m a.s.l.
- Muon Detector:
  - 30 m underground ($E_\mu > 15\,\mathrm{GeV}$)
  - Magnet (0.5 Tesla, 1000 m^3)
  - High precision drift chambers
  - T_0 detector (202 m^2 of scintillator)
  - Geom. acceptance: $\Sigma \cdot \Omega \simeq 200\,\mathrm{m^2 sr}$
  - GPS timing: 1 μs
  - Trigger and DAQ: independent of L3
- Air shower detector: 50 scint.s at surface
- Muon data: 1999-2000
  - $1.2 \cdot 10^{10}$ triggers, 12 TB data
  - $2.6965 \cdot 10^7$ seconds (312 days) live-time
- Main Topics:
  - Spectrum, point source and GRB, solar flares, composition, large area correlation, atmospheric effects, exotic events, $\overline{p}/p$ ratio

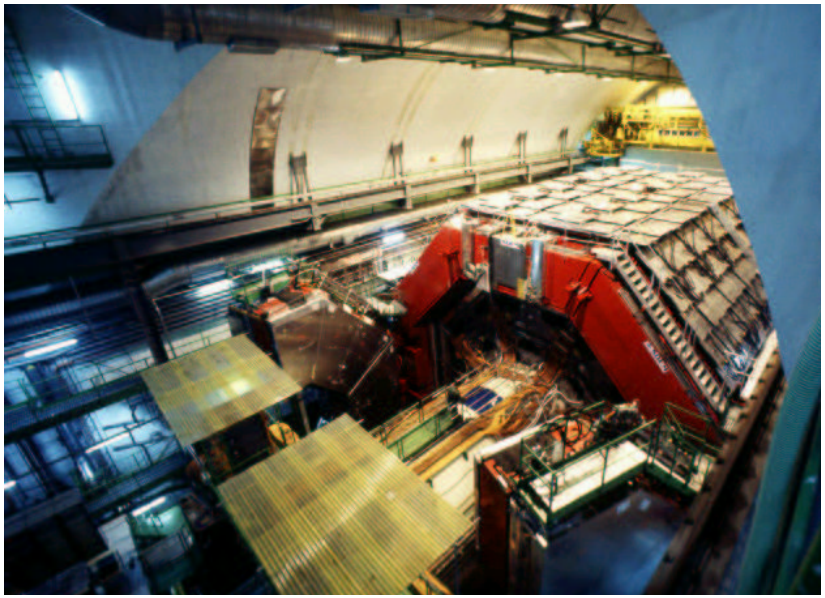

Motivation: Antiprotons in space

- The study of antiprotons (and positrons) is extremely interesting because they provide important information concerning the origin and propagation of cosmic rays in the Galaxy.
- Theoretical models
  - Secondary production: Most of the CR antiprotons observed near the Earth are secondaries produced in collisions of energetic CR particles with interstellar gas
  - Exotic sources
    - Primordial black hole (PBH) evaporation
    - Dark matter neutralino annihilation
    - High energy antiprotons from extragalactic sources ??
- Experimental Measurement
  - Direct measurement: Balloon or satellite (< 50 GeV/c)
  - Indirect method:
    - Cosmic ray μ^+/μ^- ratio (model dependent, difficult)
    - The Moon shadow technique.

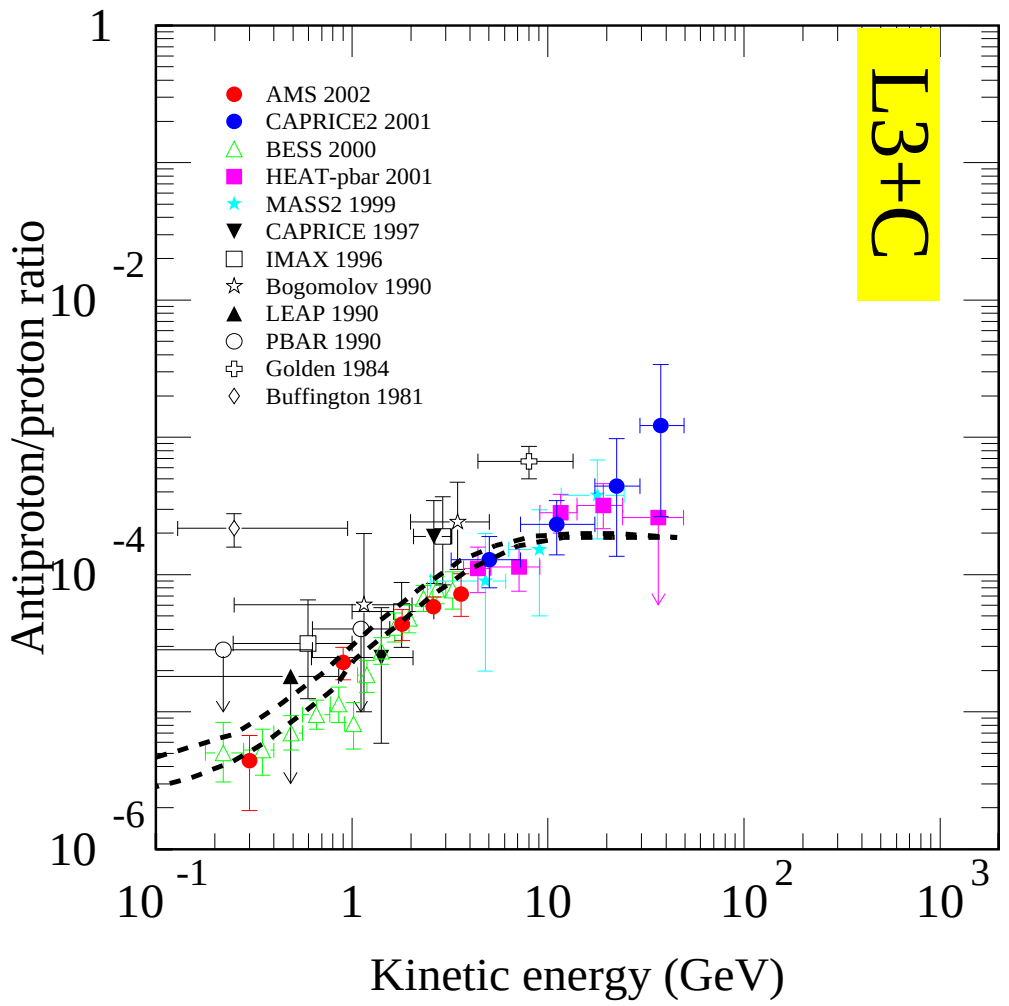

(Adapted from Boezio, M., et al., 2001, ApJ, 561, 787)

The Earth-Moon system as a spectrometer

Cosmic rays are blocked by the Moon.
$\Longrightarrow$ deficit of cosmic rays when looking at the Moon (Clark 1957).

- Size of the deficit $\longrightarrow$ effective angular resolution
- Position of the deficit $\longrightarrow$ pointing error

Geomagnetic field: positively charged particles deflected towards the East and negatively charged particles towards the West. $\Longrightarrow$ ion spectrometer (Urban et al. ARTEMIS experiment)

Observation since 1990's:

- EAS arrays: CYGNUS(only shadow), CASA(only shadow), TIBET(new data, not published)
- Imaging atmospheric Cherenkov technique(IACT): ARTEMIS(failed), CLUE(?)
- Water Cherenkov detector: MILAGRO(no limit on $\overline{p}/p$ yet)
- Muon detectors: MACRO(sun shadow, HE!), SOUDAN(no limit), L3+C

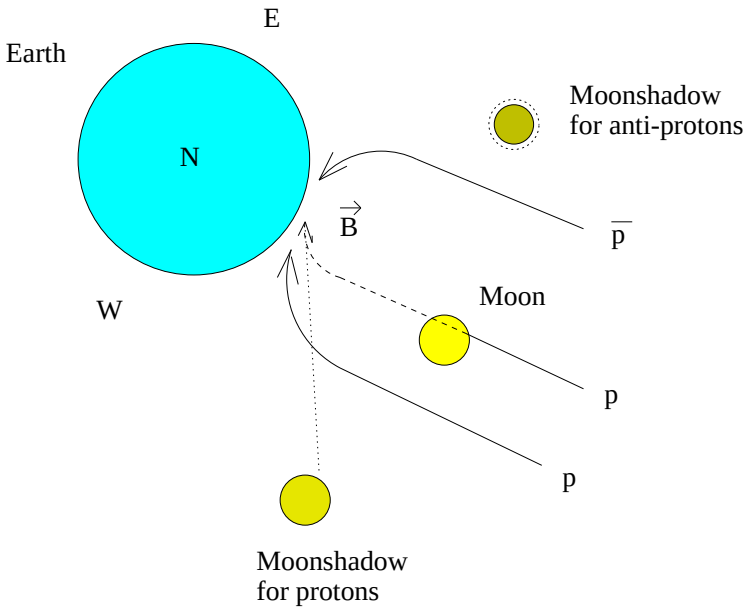

- Advantage of L3+C:
  - Excellent angular resolution and pointing
  - Precise momentum measurement
  - Low $p_{\min}$ (high rate, large deflection)
  - Real sensitivity on the earth magnetic field.

Trajectory of the Moon as seen from L3+C

- Sky seen by L3+C in the local coordinate system
  - Acceptance: $\theta_z = 0 \sim 60^\circ$
  - 1 pixel = 1 direction
  - Geomagnetic field model: IGRF
  - $\overrightarrow{\Delta\theta} = f(\alpha_z, \theta_z, \overrightarrow{p}, Z)$.
    where the parameters are direction, momentum and charge number of the primary particles.
  - The direction of deflections mainly depends on the Moon position $\Rightarrow$ the deflection coordinate system defined for each Moon position in the sky:
    - θ_{H} and θ_{V} respectively parallel and orthogonal to the computed deflection direction.

Example for a given day (215 transits observed):

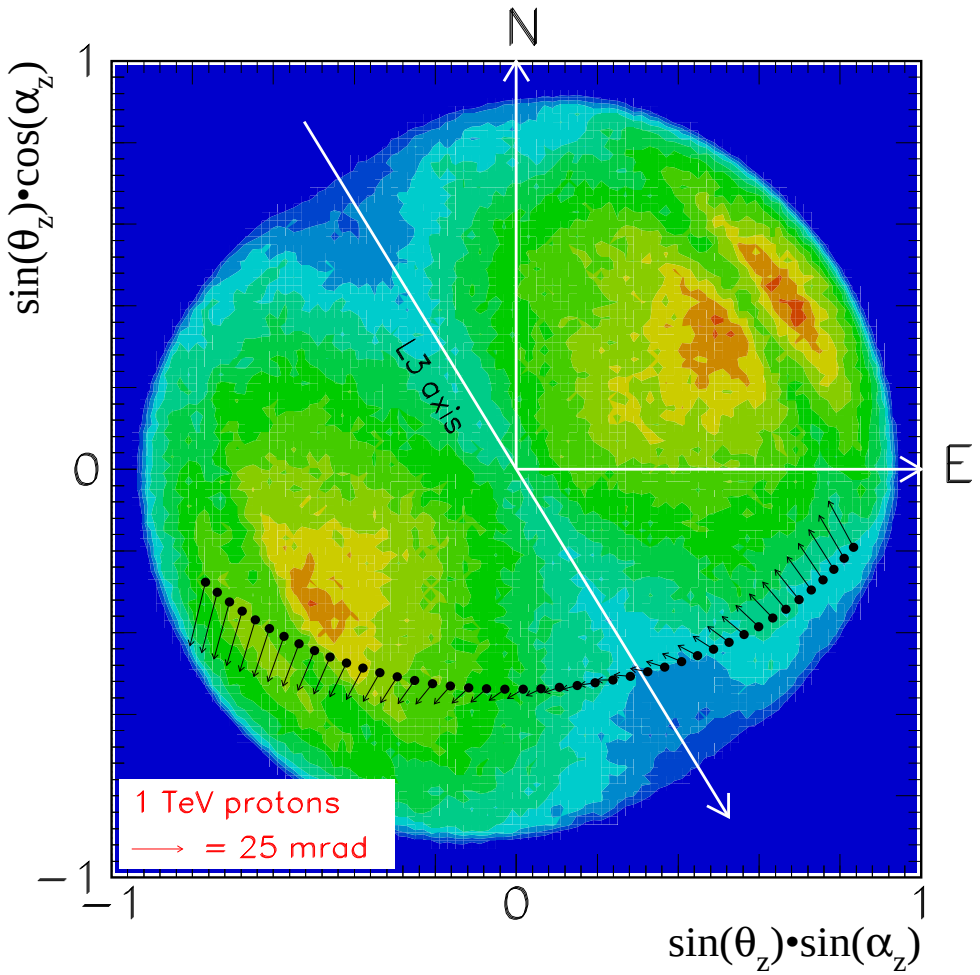

Shadow simulation

Shadow simulation in 3 different coordinate systems(local/celestial/deflection):

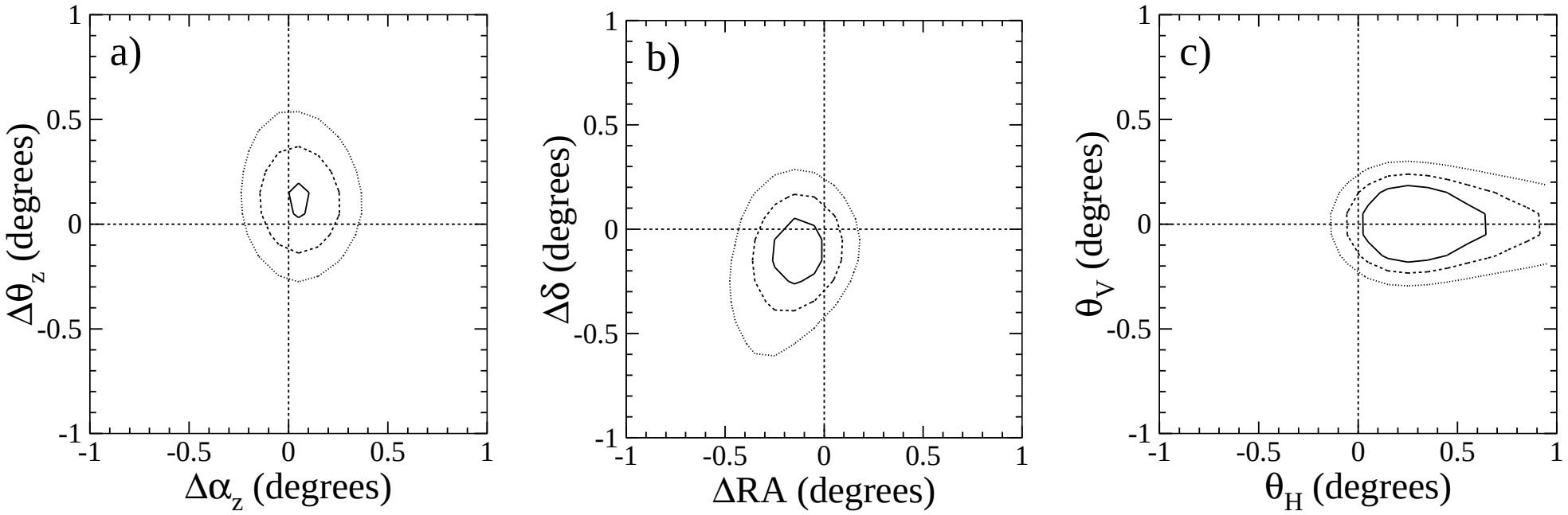

- Both the offset and elongation due to the magnetic field are more clearly visible in the deflection system.

The Angular resolution

- The effective angular resolution includes:
  - Angle between muons and primary particles
  - Multiple scattering in the molasse
  - Detector's intrinsic angular resolution
- Simulation
  - CORSIKA: air shower (confirmed by KASCADE)
  - GEANT: multiple scattering and detector response
- Double-muon events
  - nearly parallel at detector level
  - the data is in good agreement with the simulation

Single muon simulation $\Longrightarrow$ angular resolution for further analysis.

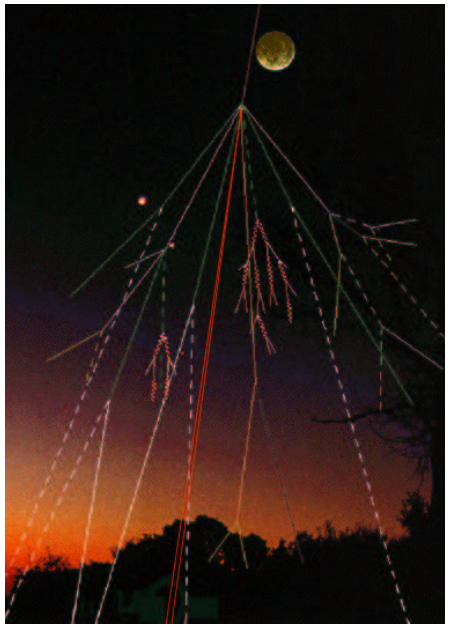

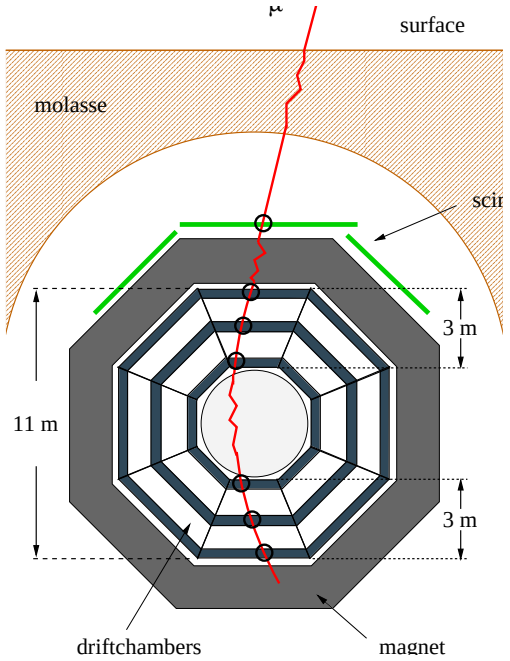

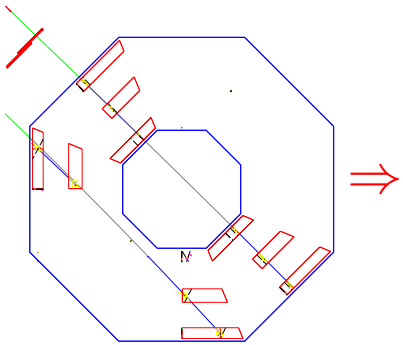

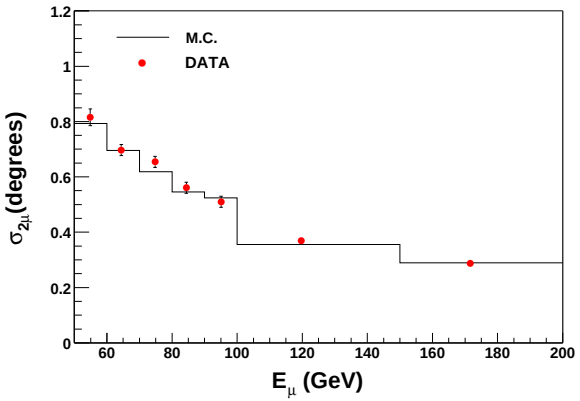

Data selection

Selection scheme:

- Only one single muon is reconstructed in each event
- The angle with the Moon direction is $< 5^\circ$
- $p_\mu >$ 50 GeV
- The zenith angle $\theta_z < 60^\circ$
- A few quality cuts

$\Rightarrow 7.35 \times 10^5$ events selected.(exposure 1557.5h, 1188.7h effective live time)

The first step:

- 1-D deficit plot
- 2-D smoothed shadow image

The fake and real Moon ($p_\mu > 100$ GeV)

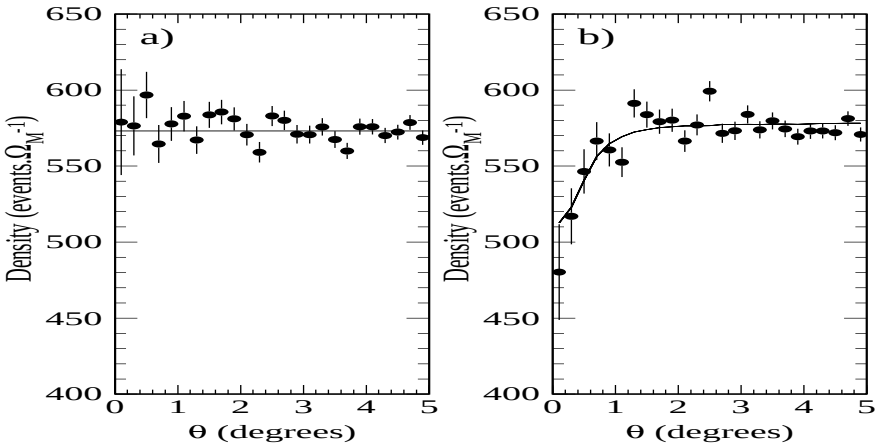

Smoothed Data:

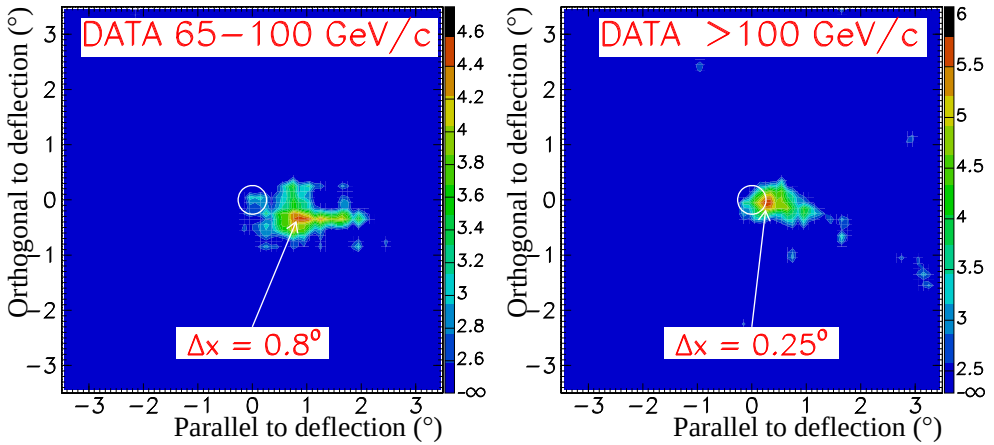

The Maximum Likelihood Method

Work on the deflection coordinate system and assume:

- A planar background;
- $\overline{p}, p$ and $^4\mathrm{He}$ have same spectral index;
- 75% muons come from protons, 25% come from heliums.

The description of the data:

$$g(x,y) = \underbrace{u_{\mathrm{x}}x + u_{\mathrm{y}}y + u_{\mathrm{z}}}_{\text{background}} - \frac{N_{\mathrm{miss}}}{1+r}[0.75\,\underbrace{f_1(x-x_0, y-y_0, \sigma)}_{p\text{ deficit}} + 0.25\,\underbrace{f_2(x-x_0, y-y_0, \sigma)}_{\text{He deficit}} + r\,\underbrace{f_1(x_0-x, y_0-y, \sigma)}_{\overline{p}\text{ deficit}}],$$

where r is the ratio of antiproton to matter,

f_1 and f_2 are the shadow functions for proton and helium respectively:

$$f(x,y) = f_{\mathrm{H}}(x) \cdot f_{\mathrm{V}}(y),$$

$$f_{\mathrm{H}}(x) = (1-c) \cdot L_1(x, a_1, b_1) + c \cdot L_2(x, a_2, b_2),$$

$$f_{\mathrm{V}}(y) = \int_{-R_{\mathrm{Moon}}}^{+R_{\mathrm{Moon}}} \frac{2}{\pi R_{\mathrm{Moon}}^2} \sqrt{R_{\mathrm{Moon}}^2 - u^2} \cdot \frac{1}{\sigma\sqrt{2\pi}} e^{-\frac{(y-u)^2}{2\sigma^2}}\, du,$$

parameters x_0 and y_0 describe the position of the deficit.

Determination of the effective angular resolution and the pointing precision

In this step no $\overline{p}$ are supposed in the primary flux.

Results obtained in the MLH fit to the matter deficit:

	$p_\mu > 100$ GeV			65 GeV $< p_\mu <$ 100 GeV		
parameter	value	uncertainty	expected	value	uncertainty	expected
N_{miss}			577.$\pm$5.			705.$\pm$6.
$x_0(^\circ)$	0.33	0.08	0.26	0.51	0.12	0.48
$y_0(^\circ)$	0.05	0.04	0.	-0.11	0.08	0.
$\sigma(^\circ)$	0.21	$^{+0.04}_{-0.03}$	0.24$\pm$0.01	0.28	$^{+0.07}_{-0.05}$	0.38$\pm$0.02
Significance	8.6		8.2	5.7		6.

Pointing error: $\leq 0.1^\circ$ for the 2 selected energy ranges.

Measurement of the $\overline{p}/p$ ratio

The antiproton search

- Select $p_\mu > 65$ GeV
- $N_{\rm miss}$ was supposed to be shared between protons, helium and antiprotons and was constrained to the expected value.
- The value of σ was also constrained to the simulated value.

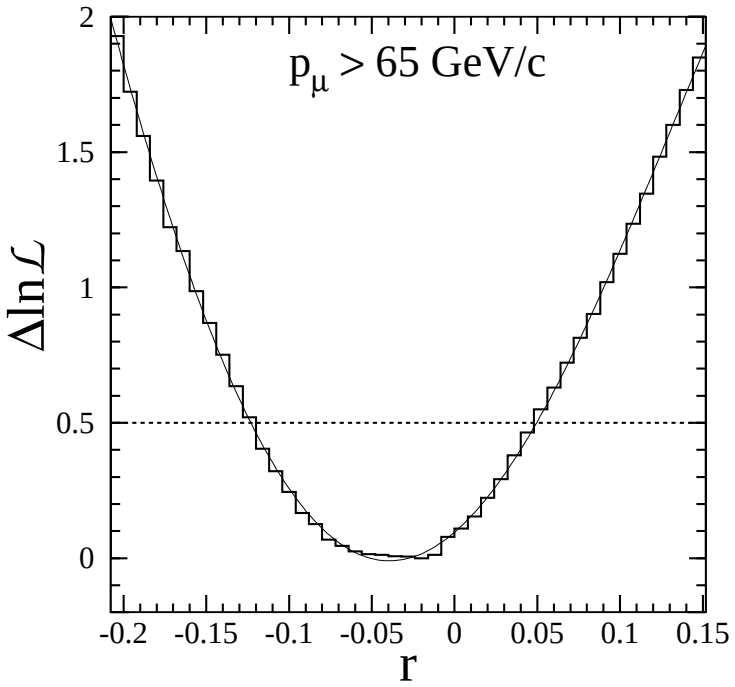

Results:

- The total significance of the deficit is 9.4 $s.d.$.
- $r = -0.04\,^{+0.09}_{-0.08}$,
  $\Longrightarrow r < 0.11$ (90% C.L.) (unified approach method. G. Feldman 1998)
  $\Longrightarrow r_{\overline{p}/p} < 0.15$ (90% C.L.) ($\frac{He}{p} \doteq \frac{0.25}{0.75}$)

Final result

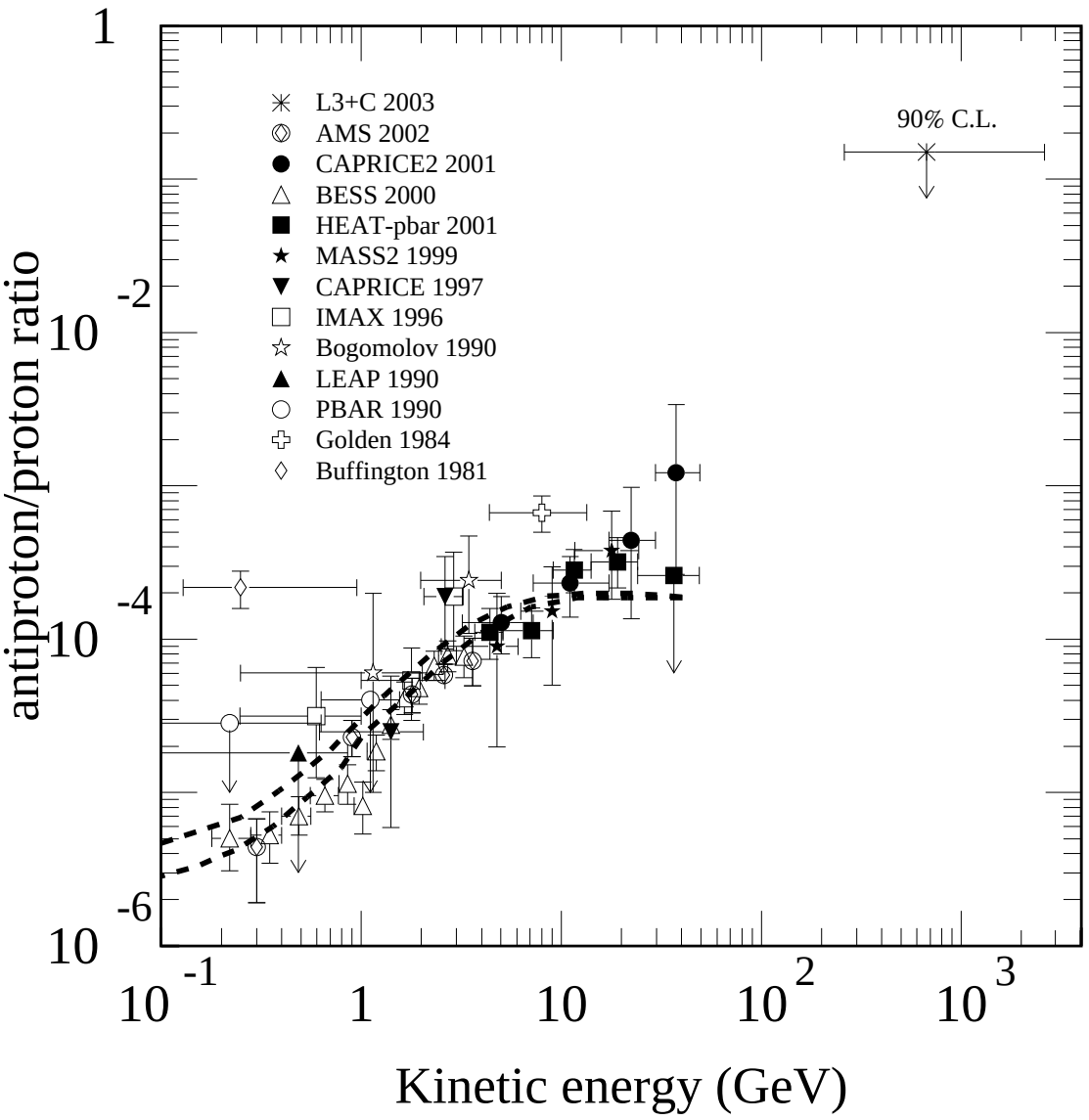

Summary

- The moon shadow has been observed with 9.4 $s.d.$ significance.
- The effective angular resolution for the set of selected events are measured to be $0.21^\circ\ ^{+0.04}_{-0.03}$ for $p_\mu > 100$ GeV and $0.28^\circ\ ^{+0.07}_{-0.05}$ for the momentum range $65 < p_\mu < 100$ GeV.
- The pointing precision is better than 0.1°.
- No event deficit on the antimatter side is observed and the upper limit of the $\overline{p}$ content is 0.11 (90% C.L.). With the assumed flux composition and antiproton spectrum, this corresponds to a $\overline{p}/p$ ratio of $r_{\overline{p}/p} = 0.15$ (primaries around 700 GeV).
- The publication is practically ready.

Outlook

- Taking into account all the accumulated data
  - At the moment only 33% of the data has been used due to restrictions in the reconstruction program.
  - A complete reconstruction of our data by a new program is currently in progress.
- New simulation scenario

$\Longrightarrow$ Improved result in the near future.

Measurement of the atmospheric muon spectrum from 20 to 2000 GeV

The muon spectrum

- Atmospheric muons are among the final products of primary cosmic ray induced air shower cascades.
- A precise measurement of the ground level muon flux can be used to estimate the primary flux, the primary composition and to study the hadronic interactions involved in the production of the muons' parent mesons.
- It provides a crucial input to the theoretical calculation of the atmospheric neutrino flux, because each muon is produced with an accompanying muon neutrino. This is needed to interpret the observed muon neutrino flux deficit at high energy and to evaluate the background for neutrino astronomy.

The muon spectrum

- L3+C measured
  - the vertical muon flux 20-2000 GeV
  - the charge ratio 20-600 GeV
  - the zenith angle dependencies up to 58°
- Large exposure factor of about $180\,\mathrm{m}^2\,\mathrm{sr}\,\mathrm{d}$
- Maximum detectable momentum at 4.7 ± 0.4 TeV
- Minimum systematic error of vertical muon flux is 2.6%

Vertical muon spectrum and charge ratio ($\cos(\theta) > 0.975$)

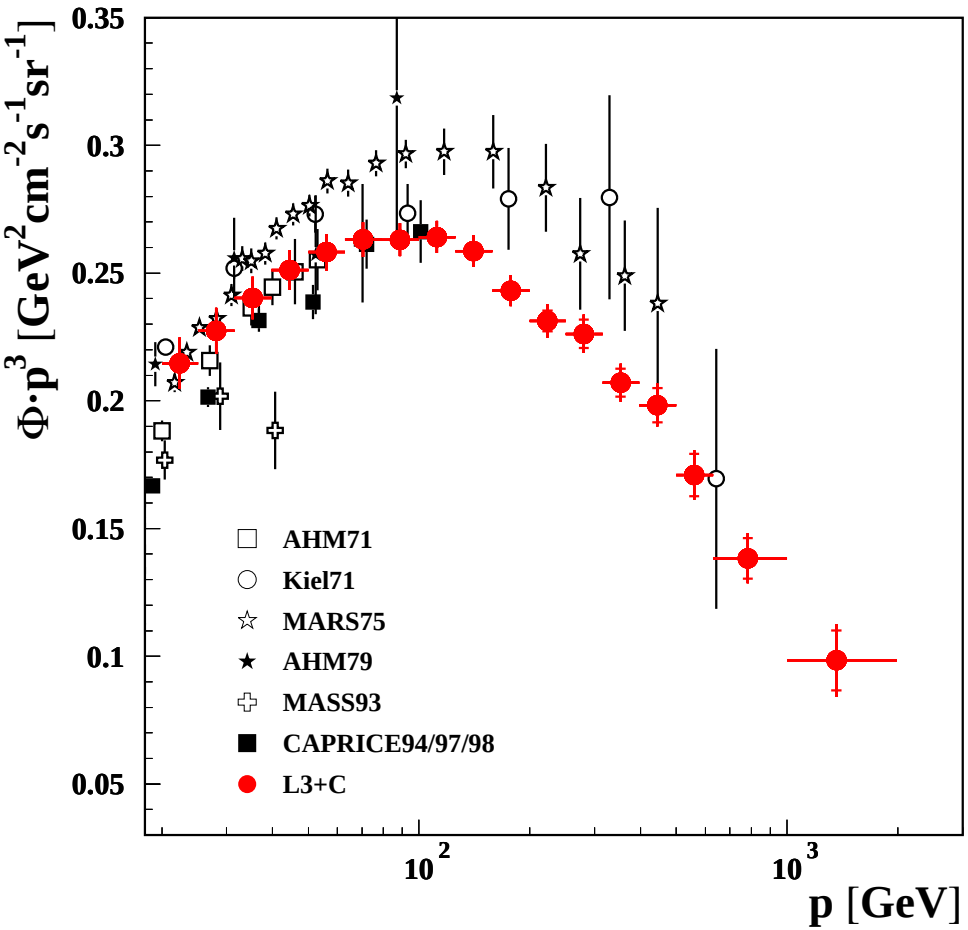

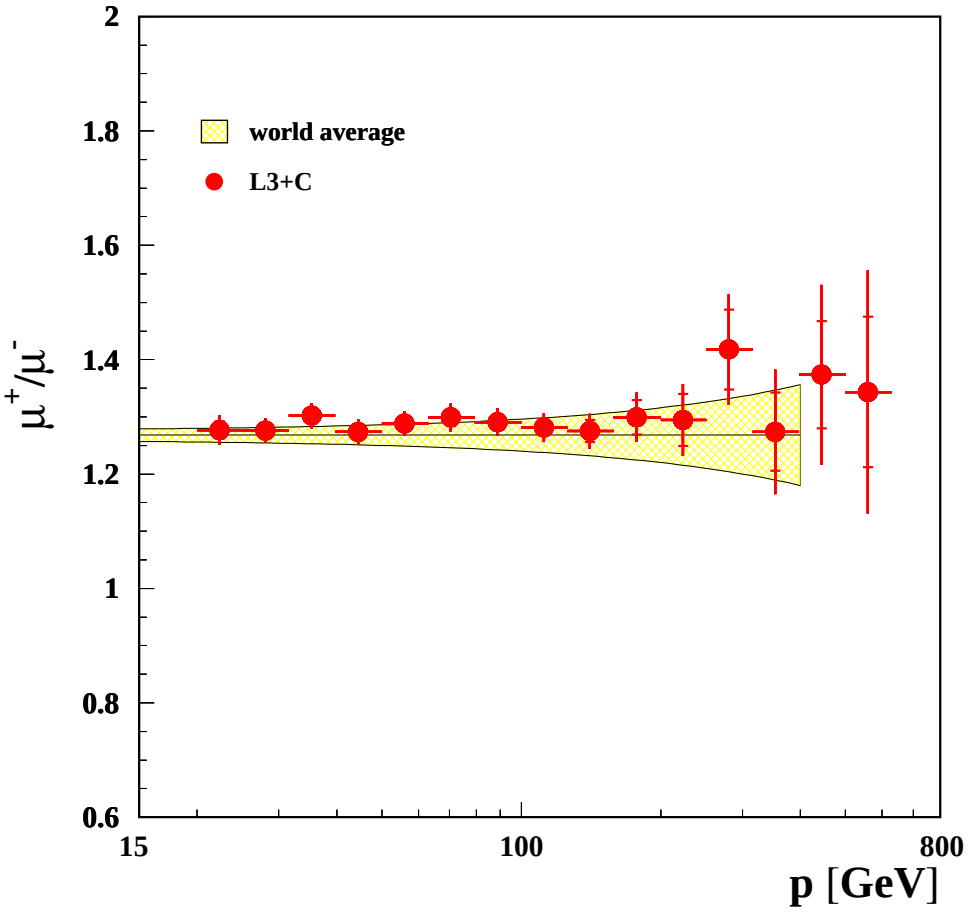

- Comparison is made with other experiment results providing obsolute flux values.

(inner error bar: statistical error; full error bar: total error)

Zenith angle dependence

muon spectrum

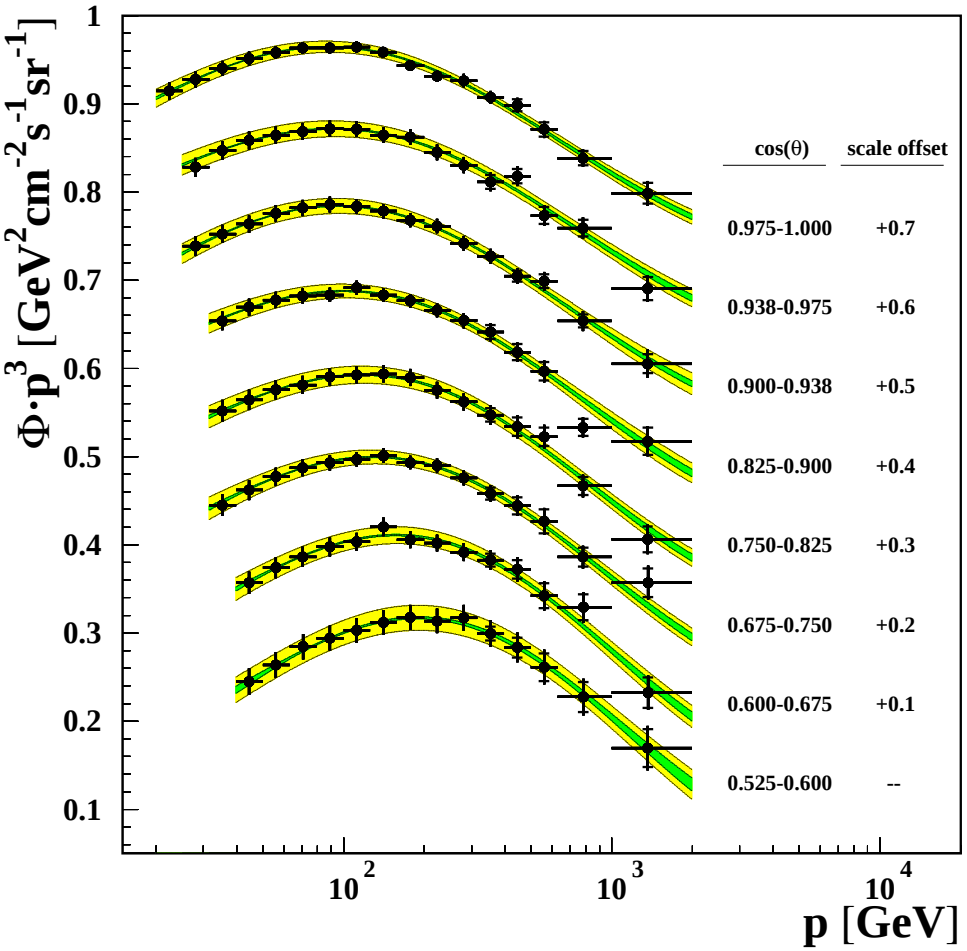

charge ratio

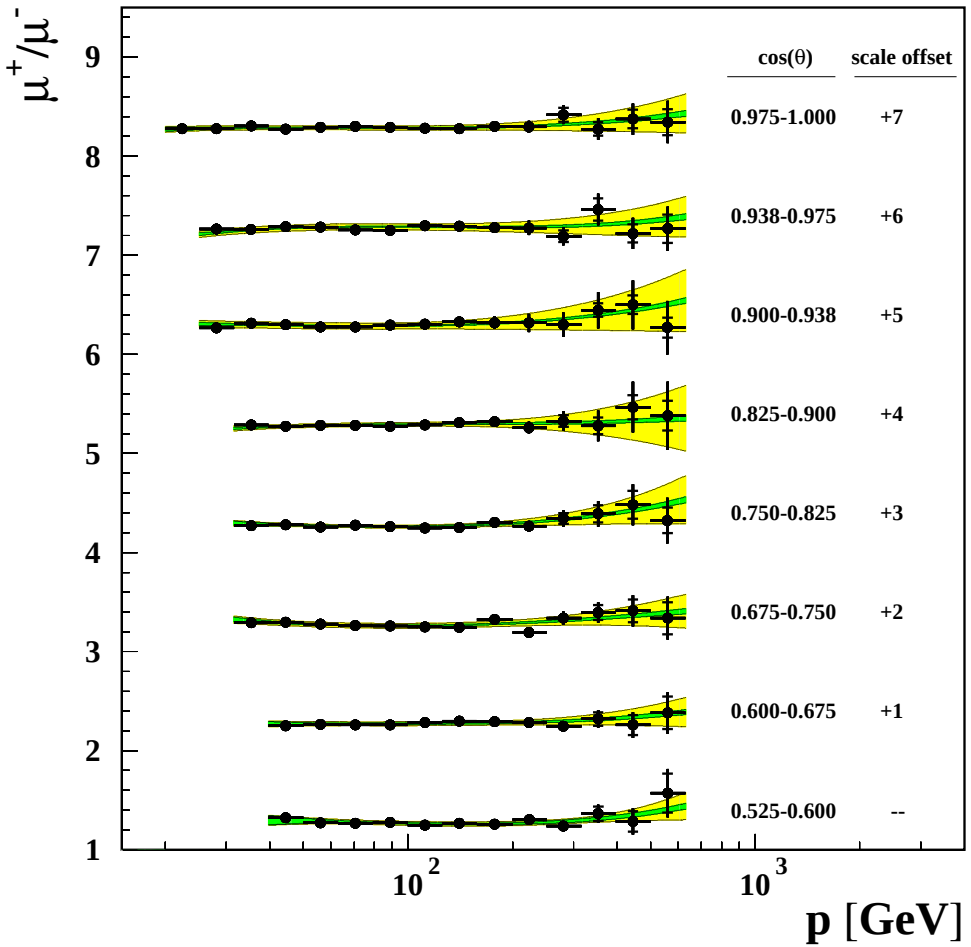

Comparison with TARGET 2.2 - a hadronic interaction modes

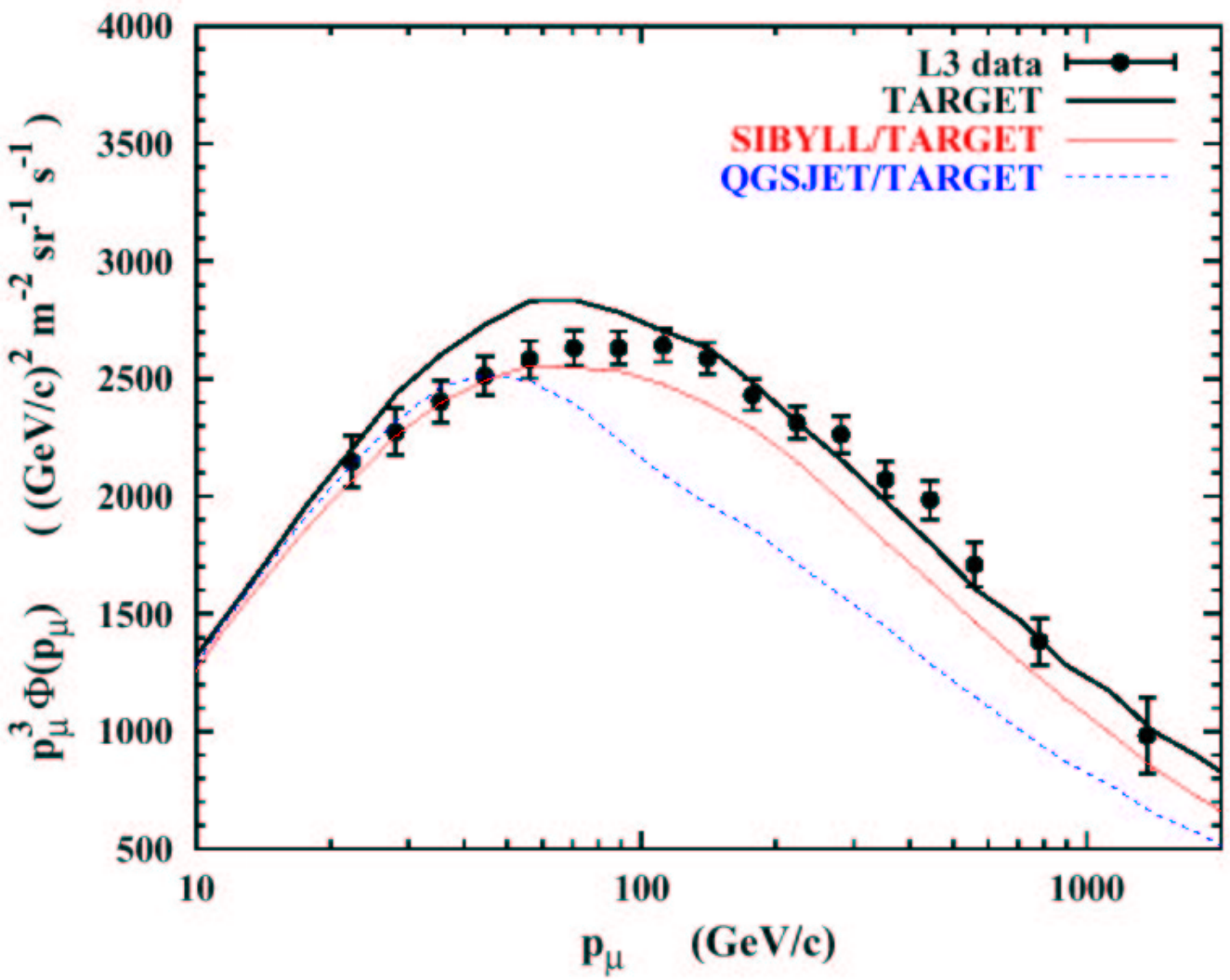

Fig. 3. Comparison of inclusive muon flux predictions to L3 data [17]. Shown are calculations using QGSJET 98 [15], SIBYLL 2.1 [7] and TARGET as high-energy hadronic interaction model.

(R. Engel et al., Proc. 28th ICRC, Tsukuba, Japan, (2003) 1603)